J Ind Microbiol Biotechnol (2013) 40:1263–1271
DOI 10.1007/s10295-013-1321-3

SIMB
Society for Industrial Microbiology and Biotechnology

Scalable economic extracellular synthesis of CdS nanostructured particles by a non-pathogenic thermophile

Ji-Won Moon · Ilia N. Ivanov · Chad E. Duty · Lonnie J. Love · Adam J. Rondinone · Wei Wang · Yi-Liang Li · Andrew S. Madden · Jennifer J. Mosher · Michael Z. Hu · Anil K. Suresh · Claudia J. Rawn · Hyunsung Jung · Robert J. Lauf · Tommy J. Phelps

Received: 16 April 2013 / Accepted: 3 August 2013 / Published online: 5 September 2013

Abstract We report microbially facilitated synthesis of cadmium sulfide (CdS) nanostructured particles (NP) using anaerobic, metal-reducing *Thermoanaerobacter* sp. The extracellular CdS crystallites were <10 nm in size with yields of ~3 g/L of growth medium/month with demonstrated reproducibility and scalability up to 24 L. During synthesis, *Thermoanaerobacter* cultures reduced thiosulfate and sulfite salts to H_2S, which reacted with Cd^{2+} cations to produce thermodynamically favored NP in a single step at 65 °C with catalytic nucleation on the cell surfaces. Photoluminescence (PL) analysis of dry CdS NP revealed an exciton-dominated PL peak at 440 nm, having a narrow full width at half maximum of 10 nm. A PL spectrum of CdS NP produced by dissimilatory sulfur reducing bacteria was dominated by features associated with radiative exciton relaxation at the surface. High reproducibility of CdS NP PL features important for scale-up conditions was confirmed from test tubes to 24 L batches at a small fraction of the manufacturing cost associated with conventional inorganic NP production processes.

Keywords CdS nanostructured particles · Nanobiotechnology · Thermoanaerobacter · Fermentation · Photoluminescence · Scalable synthesis

Introduction

Electro-optical properties of nanostructured particles (NP) including semiconducting quantum dots have been applied

J.-W. Moon (✉) · A. K. Suresh · H. Jung · R. J. Lauf · T. J. Phelps
Biosciences Division, Oak Ridge National Laboratory (ORNL), Oak Ridge, TN 37831, USA
e-mail: moonj@ornl.gov

I. N. Ivanov · A. J. Rondinone
Center for Nanophase Materials Sciences, ORNL, Oak Ridge, TN 37831, USA

C. E. Duty · C. J. Rawn
Materials Science and Technology Division, ORNL, Oak Ridge, TN 37831, USA

L. J. Love
Measurement Science and Systems Engineering Division, ORNL, Oak Ridge, TN 37831, USA

W. Wang
Environmental Sciences Division, ORNL, Oak Ridge, TN 37831, USA

Y.-L. Li
Department of Earth Sciences, The University of Hong Kong, Hong Kong, China

A. S. Madden
School of Geology and Geophysics, University of Oklahoma, Norman, OK 73019, USA

J. J. Mosher
Stroud Water Research Center, Avondale, PA 19311, USA

M. Z. Hu
Energy and Transportation Science Division, ORNL, Oak Ridge, TN 37831, USA

Present Address:
A. K. Suresh
Department of Molecular Medicine, City of Hope, 1500 East Duarte Road, Duarte, CA 91010, USA

toward solid state lighting [17], photovoltaic devices [11], and biological labeling [2]. Current approaches for synthesizing NP include colloidal synthesis using organic solvents [7], solvothermal routes requiring temperatures in excess of 180 °C for more than 24 h [8], or thermolysis which may require multiple steps and an energy intensive process including calcination at high temperature [31]. In most synthesis techniques, sub-gram quantities of nanocrystals are produced, as conventional synthetic routes are limited to small-scale reactions [5]. Recently, efforts for large-scale NP synthesis (>1 g) were initiated using organically passivated materials with a narrow size distribution [15]. The search for scalable and environmentally friendly NP synthesis that also overcomes cost and scaling limitations of chemical synthesis has attracted significant attention [28].

Nano-biotechnology, an emerging field of science, offers the use of organisms [29] for synthesizing cadmium sulfide (CdS) nanoparticles. Microbial biosynthesis of CdS NP can offer several advantages—making NP synthesis scalable, low cost, and environmentally friendly [20]. The formation of CdS has been found to be compatible with microbial mechanisms of heavy metal tolerance and enzymatic mechanisms converting metal ions into precipitates [6]. Previous examples of cadmium detoxification by precipitation included the formation of CdS either on the surface of *K.pneumoniae* [28] or inside cells of engineered *E.coli* [13, 18], and peptide-capped intracellular CdS particle formation within living *Schizosaccharomyces pombe* yeast cells [23]. Although CdS NP were observed in these studies, characterization of their optical properties was limited due to small NP yields. The low yield of previously biosynthesized NP was in part due to limited numbers of cells and the product recovery, which required cell lysis followed by NP purification [13].

The cost of CdS NP production can be compared based on the price of the components. The price of sulfur sources vary widely from $1,600/kg for H_2S to $86/kg for Na-thiosulfate and $40/kg for Na-sulfite (Sigma-Aldrich, Milwaukee, WI, USA). Competitive manufacturing cost of the biological process uses less expensive oxidized sulfur sources, while chemical syntheses requires reduced sulfur compounds at a higher price. Using a more oxidized form such as thiosulfate or sulfite can produce CdS NP at around 5 % of the cost compared to chemical synthesis requiring expensive reduced species such as Na_2S and H_2S.

Here, we report the microbially facilitated synthesis of extracellular CdS NP with controlled size, crystal structure, and optical properties using an advantageous low cost and environmentally friendly process that appears inherently scalable at yields approaching 3 g/L/month.

Materials and methods

Synthesis of CdS NP

Extracellular CdS NP were produced using thermophilic metal reducing bacteria, *Thermoanaerobacter* sp., such as TOR-39 [16] or X513 [26], which are not sulfate-reducing bacteria. Results shown here were obtained with *Thermoanaerobacter* sp. X513. The CdS NP synthesized using *Desulfovibrio desulfuricans*, G20, a metal and sulfate-reducing bacterium [34] and inorganically synthesized CdS NP from Cd salt and sodium sulfide were used as reference materials.

The CdS NP synthesis was initiated with the inoculation of 10 mM glucose, 2 % volume of mid-log phase growth of X513 culture plus 10 mM of a sulfur source such as thiosulfate or sulfite added to a modified TOR-39 media at 65 °C [22], which kept bicarbonate concentration low so as to prevent otavite ($CdCO_3$) precipitation. After 1 to 4 days of incubation aliquots of cadmium chloride (0.4–1.6 mM/day) were dosed a single time for high impact or ten times via pulsed dosing to produce CdS NP. Screening the Cd^{2+} toxicity revealed that dosing at 0.01 mM proved inhibitory to growth by 91 % loss of optical density and dosing at 0.05–0.5 mM lost more than 97 % compared to the control sample without Cd^{2+} after 24 h. More than 1 mM resulted in lower optical density than the background of sterile growth medium. Control experiments without microbes were performed at pH 6.96 for thiosulfate and pH 7.01 for sulfite in the same growth medium incubated with X513 for 24 h. Both samples were incubated with the same pulsed dosing of 0.4 mM Cd^{2+} at 65 °C.

Cultured samples were incubated for another 24 h after the final dosing and harvested. Culture medium volumes varied from 10 mL to 24 L with the same dosing ratio and the Cd concentration was increased in the same medium volume for mass production. The total effect of incubation time and dosing methods was evaluated. Some samples were centrifuged in an anaerobic glove bag (Coy, Ann Arbor, MI, USA) to remove background effects of medium and kept reduced with 0.2 mL of 11.5 mM Na-dithionite. The CdS NP products were washed with deionized water and centrifuged five times. After each centrifugation, cell pellets were readily removed from the denser NP by scraping. After five washes microscopic cell counts were reduced more than three orders of magnitude while the sodium concentration of the suspension was similarly reduced from 2000 mg/L to 5 mg/L. Aliquots of the CdS NPs were mixed with methanol and the slurry was applied to a silicon zero background plate for X-ray diffraction (XRD) analysis.

Characterization

After cooling withdrawn samples, the final pH and Eh of bacterial cultures and controls were measured in an anaerobic chamber using combination pH and Eh electrodes [22]. Dissolved sulfur species in the medium such as sulfite and thiosulfate were diluted with degassed deionized water, and then measured by an ion chromatograph equipped with a conductivity detector (DX-120, Dionex, Sunnyvale, CA, USA). The concentrations of dissolved hydrogen sulfide species including H_2S and HS^- were measured by colorimetry [4]. Carbon dioxide and hydrogen sulfide gases in the headspace were collected using a gas-tight syringe and analyzed on an Agilent 5850 gas chromatograph (Agilent Technologies, USA) equipped with a thermal conductivity detector as described previously [19]. The protein concentration was measured before Cd^{2+} dosing with a BCA™ protein assay kit (Pierce, Rockford, IL, USA) using bicinchoninic acid and the calibration curve was obtained using albumin as a standard.

Absorption properties were measured using samples directly extracted from the culture vessel using a syringe and analyzed using a UV-vis spectrophotometer (HP 8453, Hewlett-Packard). Photoluminescent (PL) properties of NP were measured using a fluorescence spectrometer (JY Horiba, Spex). The fluorescent luminance (FL) measurement was performed with a washed, stored NP suspension reduced with 0.2 mL of 11.5 mM Na-dithionite and prepared with degassed deionized water to adjust the extracted volume prior to the measurements. The PL of solid NP powders (deposited on glass slides) was measured with the sample positioned at 30° to the excitation beam with 5 nm slits on excitation and emission monochromators and 0.1 s integration time. The excitation was with a 400 nm light.

An X-ray diffractometer (X'pert PRO, PANanalytical, Natick, MA, USA) equipped with Cu–Kα radiation at 45 kV/40 mA from 10°–70° 2θ was used to obtain XRD profiles. Data were analyzed by profile fitting without any structural parameters using the JADE software package (Material Data Inc.) following previous research [21]. Average crystallite size was determined using the JADE software along with the Scherrer equation. Transmission electron microscopy (TEM, FX 2000, JEOL, Japan) was used to examine the morphology and grain size of the precipitated NP.

Results and discussion

The effect of microbes and sulfur sources on crystal phases of CdS NP

Incubation of metal-reducing X513 with 10 mM thiosulfate or sulfite as electron acceptors resulted in production of ≥6 mM sulfide which reacted with cadmium salt concentrations of 4.45 mM or 8.90 mM (with pulsed dosing of 0.45 and 0.89 mM/day, respectively). After 10 days XRD patterns (Fig. 1**a**, **b**) revealed CdS NP in polymorphic phases of cubic hawleyite and hexagonal greenockite (Fig. 1**c**). The TEM micrographs of CdS NP (Fig. 1**e**)

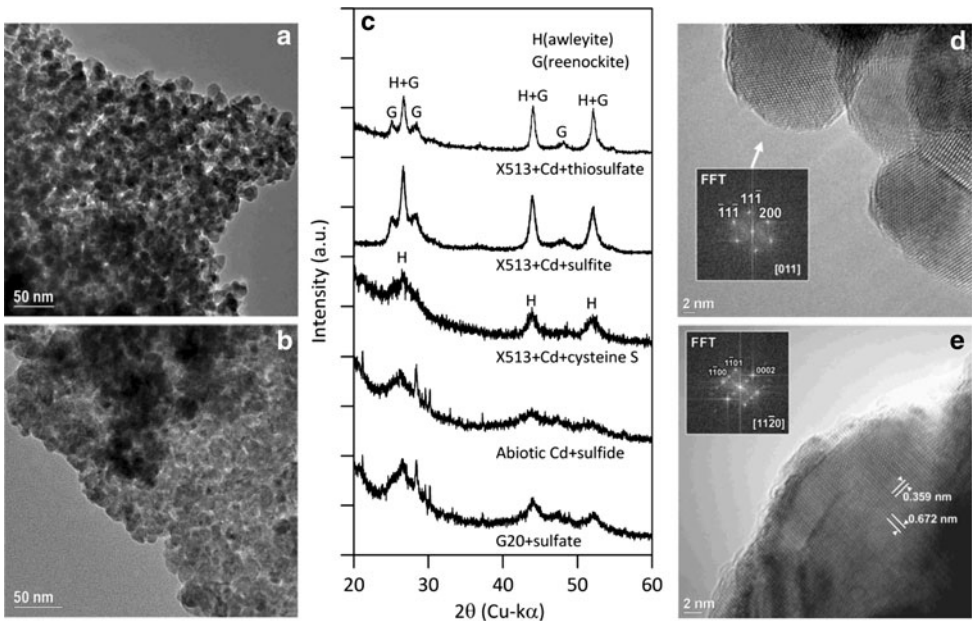

Fig. 1 **a**, **b** TEM micrographs of CdS cultured with X513 after 4.5 and 8.9 mM of pulsed dosing with Cd^{2+}, respectively; **c** XRD patterns of CdS NP final products with differing sulfur sources and microbes; **d**, **e** co-existence of cubic hawleyite phase (**d**) and hexagonal greenockite phase (**e**) of CdS NP

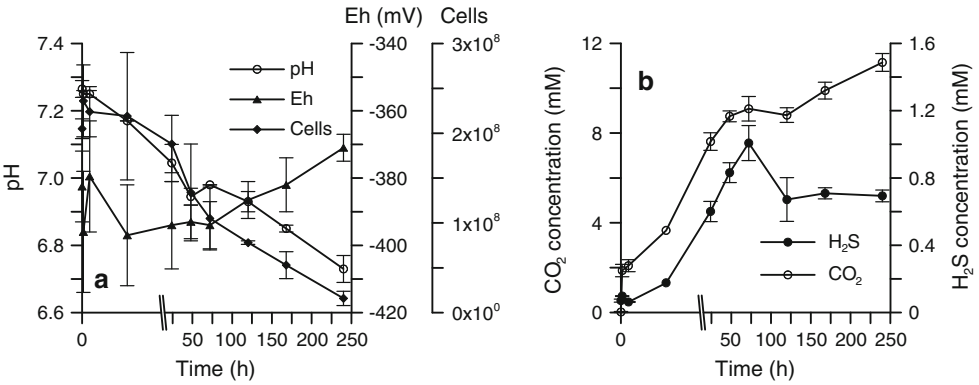

Fig. 2 Time course experiment synthesizing microbially mediated CdS NP via pulsed dosing of cadmium precursor salts ($t = 0$ when Cd dosing started). **a** pH and Eh of the culture medium and numbers of live cells; **b** H_2S and CO_2 concentration in the headspace

produced from thiosulfate exhibited a clear crystal pattern with 0.359 and 0.672 nm spacing corresponding to (100) and (002) that was in agreement with the hexagonal crystal structure. Fast fourier-transforms of lattice fringe spacings of CdS NP were consistent with cubic and hexagonal structures (Fig. 1**d**, **e**). Only the cubic hawleyite phase (Fig. 1c) was found in CdS NP when a cysteine sulfur source was used. Abiotic controls using Cd salts and sodium sulfide, and a biological method with *Desulfovibrio desulfuricans*, G20 cultures with sulfate, produced the cubic phase but not the hexagonal crystal structure. Cadmium (sulfate) hydroxide and/or cadmium carbonate were observed as impurities in G20 and abiotic samples. Control samples without microbes showed negligible precipitation.

The mechanism of CdS NP formation

Test tubes with 10 mL medium were prepared in duplicate for the incubation of X513 with 10 mM glucose and 10 mM thiosulfate for 24 h, after which 0.4 mM/day $CdCl_2$ was dosed as a discrete pulse for 10 days. The aliquots of CdS NP were sampled nine times between 5 min and 240 h. The formation of CdS NP was apparent by an immediate color change from colorless to yellow upon Cd^{2+} dosing, indicating a reaction between Cd^{2+} and the reduced sulfide species from microbially mediated reduction of thiosulfate.

Cultures with X513 produced significant amounts of organic acid and CO_2 by the metabolic activity [39] which increased acidity. As a result, decreases of live cell counts and an increase in redox potential were observed after $t = 0$ (Fig. 2**a**). Continuous microbial activity throughout the experiment was evidenced by the accumulation of CO_2 gas in the headspace. Concentration of H_2S above the fermented medium stabilized to a relatively constant level after 100 h (Fig. 2**b**). The results demonstrated that the extracellular formation of CdS NP was the result of the reaction of microbial reduction of the sulfur source to sulfide followed by its reaction with Cd^{2+} cations. The CdS formation was the thermodynamically favored reaction in that the free energy of formation of CdS by $[Cd^{2+} + H_2S = CdS + H_{2\ (g)}]$ or $[Cd^{2+} + HS^- = CdS + H^+]$ was estimated to be −46.3 and −68.3 kcal, respectively [33]. One mechanism in the microbially facilitated synthesis of CdS NP is the reducing force of the microbial activity which transfers electrons from glucose as an electron donor to adjacent thiosulfate as a terminal electron acceptor. Factors causing pH drop can be acetate formation from glucose, dissolution of CO_2 into HCO_3^- at neutral pH, conversion of H_2S gas to dissolved hydrogen sulfide species HS^-, incorporation of Cd^{2+} with HS^- to precipitate sparingly soluble CdS NP, and combinations of any of these.

Control experiments without microbes with pH drop showed no precipitation. Without microbial activity, there was no driving force to reduce intermediate sulfur sources to sulfide species to react with Cd^{2+} thermodynamically under the same temperature and pH condition.

Another mechanism of CdS NP formation is the catalytic nucleation on the cell membrane combined with the reducing force. A comparison study was conducted with 24 h incubated samples of X513 only with thiosulfate and glucose (as pristine), 2 h-autoclaved, and filtered using 0.2 μm filter in the glove bag. Only a 0.6 % fraction of the protein remained after filtering from pristine samples. They exhibited little differences of pH–Eh conditions at room temperature before dosing with Cd^{2+} (Fig 3**a**). Samples incubated for 30 h were also tested as pristine and filtered, because approximately 50 % of the sulfide was lost during filtering or to volatilization or adsorption (Fig 3**b**). The Cd^{2+} was dosed at room temperature for 30 min and 3 h. A short reaction time (5 min) generated a broad recombination peak in the red-region (Data not shown).

Incorporation of Cd^{2+} and reduced sulfide with live or dead cells produced expected FL emission peaks at 515 nm (Fig 3**c**), but the filtered sample exhibited some variance; (1) very small peak at 515 nm or (2) only broad emission peak in the red region with higher intensity. Autoclaved samples with dead cells showed a slight blue-shift. The reason is not certain, but one possibility is that the 2 h-

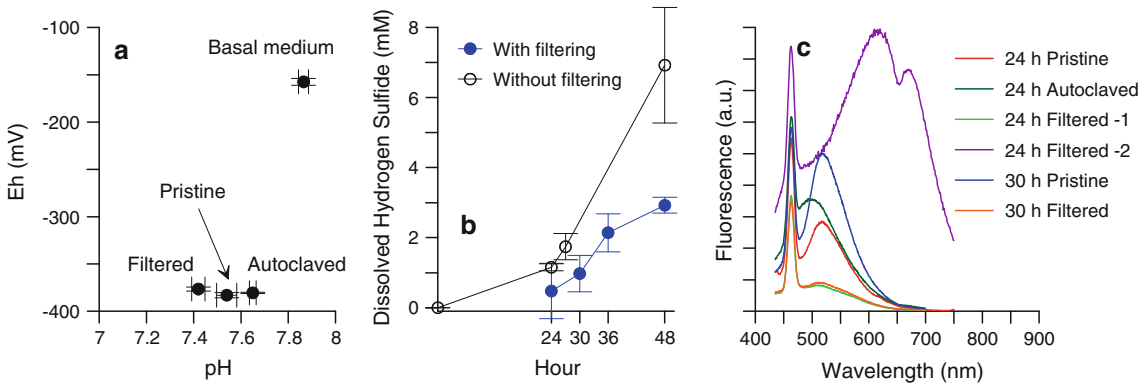

Fig. 3 Comparison study among pristine, autoclaved, and filtered samples. **a** pH–Eh condition before Cd^{2+} dosing; **b** dissolved hydrogen sulfide concentration of pristine and filtered samples for 48 h incubation; **c** FL peaks came from precipitates after dosing Cd^{2+} and 463 nm peak came from deionized water

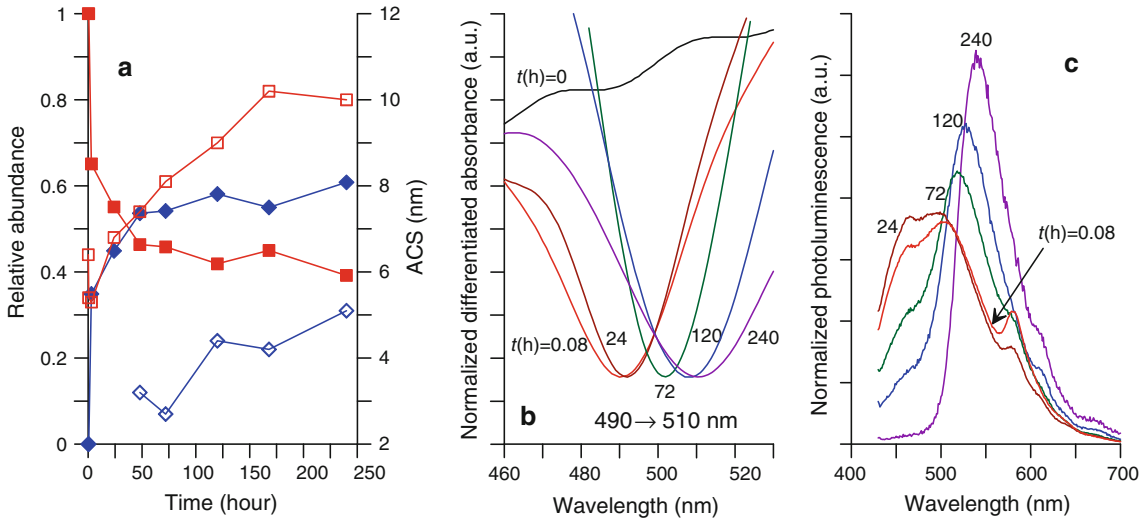

Fig. 4 Time course experiment to synthesize microbially mediated CdS NP via pulsed dosing of Cd^{2+} ($t = 0$ when Cd dosing started). **a** semi-quantification of relative abundance (solid) and average crystallite size (open) of cubic hawleyite (*square*) and hexagonal greenockite (*diamond*); **b** absorption peaks shift from 490 to 510 nm; **c**, FL peaks shift from 505 to 540 nm (excitation at 400 nm)

autoclaving process resulted in breakdown of cells, that in turn increased the specific surface area with increased cell debris and increased nucleation sites. It was concluded that the combined reduction driving force by microbial activity and catalytic nucleation are responsible for CdS NP production in our microbially facilitated synthesis.

Impact of incubation time on the structure of CdS NP

The CdS NP precipitates from a time course experiment in Sect. 3.2 were also examined to discern the impact of incubation time on the CdS NP structures. The XRD analysis indicated a transition (after 24 h of incubation) from cubic to a mixture of cubic and hexagonal phases until the end of the experiment at 240 h (Fig. 4**a**). Relative abundance between the two phases was obtained using reference intensity ratios [3]. After 24 h of incubation, XRD analysis distinctively revealed the formation of the hexagonal phase as indicated by (002) and (102) peaks at about 26.4° and 28.1° 2θ, respectively, in addition to the cubic phase. After 240 h of incubation, the CdS NP contained a larger fraction of the hexagonal phase. Until 24 h, the average crystallite size of the precipitated cubic phase was about 5 nm without additional supply of $CdCl_2$, but increased to 7 nm at 48 h with an additional dose. It was in agreement in that CdS was previously obtained from hexagonal-phased nucleation seeds under high temperature conditions (~300 °C) and cubic-phased seeds dominated at lower temperatures (~120 °C) [12].

Nucleation of less thermodynamically stable cubic phase followed by the recrystallization of more stable

Table 1 Variation of ACS, conversion efficiency, and yield according to different dosing regimes, and incubation times with 1L medium scale in duplicates with 2 % X513 inocula of mid-log phase growth

Series	Dosing		Incubation (day)			ACS (nm)	CE (%)	Yield (g/L/month)
	Con (mM/day)	Times	Enrichment	Inoculation	Aging			
S-1	0.4	1	2	10	0	7.8 ± 0.3	99.7 ± 3.9	1.44 ± 0.06
S-2	0.8	1	2	10	0	7.2 ± 0.1	82.2 ± 1.2	2.37 ± 0.03
S-3	0.8	2	2	4.5	0	5.7 ± 0.1	69.9 ± 4.7	3.73 ± 0.25
S-4	0.8	2	2	4.5	5	6.1 ± 0.4	88.7 ± 3.5	2.67 ± 0.10

Con concentration, *ACS* average crystallite size, *CE* conversion efficiency

hexagonal phase correlates well with the Ostwald's step rule [24] which implies that the cubic phase probably has a lower interfacial free energy than the hexagonal phase. The observed changes in the crystal structure of CdS NP can also be explained using a phase stability reversal mechanism previously reported for thermal and photochemical synthesis of CdS nanoparticles [10]. This mechanism has been suggested for the 3 nm sized cubic phase [1] and the 100 nm size of the hexagonal phase [35] of CdS formed via thermal and photochemical reduction, respectively. In our case, chelation of organic acid byproducts on the surface of CdS NP could cause significant changes of surface free energy of the NP [27] facilitating accumulation of the hexagonal phase.

Size-dependent optical properties of CdS NP were confirmed by red-shifts of absorption and FL spectra (Fig. 4**b**,**c**). Absorption spectra did not show well-resolved peaks; therefore, the inflection points from patterns were obtained after smoothing and differentiation of absorption spectra. Acquired absorption peaks that were shifted from 490 to 510 nm correlated well with the dosing amount of Cd^{2+} and incubation time as well as average crystallite size obtained from XRD.

The FL of the CdS NP in the time course experiment with a pulsed dosing showed the red shift from 505 to 540 nm (excitation at 400 nm) which correlated well with the change in average crystallite size (ACS) from 5 to 11 nm. The red shift of both the absorption and the FL spectra can be ascribed to weak dielectric confinement [30] induced by increased ACS, as a result of increased dosing of Cd^{2+}. The ACS of the cubic phase CdS determined from TEM images were 17.1 ± 6.6 nm ($N = 156$) that was comparable to the ~11 nm diameter estimated from XRD measurements. The ACS of hexagonal phase CdS was found to be 49.9 ± 29.9 nm ($N = 104$), significantly larger than the ~ 10 nm estimated from XRD. The difference between TEM and XRD derived ACS might be due to oriented aggregation of the CdS. Crystallographically driven aggregation of NP seeds has been observed in other sulfide systems [14]. Each smaller CdS in the aggregates could serve as a coherent scattering domain for X-rays.

The effect of medium volume, biomass, and dosing concentration on scalability of CdS NP production

Nucleation and growth of CdS NP also depended on incubation time, dosing concentration, and initiation time of dosing with subsequent H_2S development. For example, using 1 L-scaled medium, 7.8, 7.2, and 6.1 nm ACS of CdS NP were synthesized with pulsed dosing of 0.4 mM/day, 0.8 mM/day for 10 days and 1.6 mM/day for 5 days indicating smaller crystallite sizes with increased dosing concentrations (Table 1). The average crystallite size of CdS NP increased with longer incubation times with 0-and 5-days aging producing 5.7 and 6.1 nm, respectively (Table 1). Another batch initiated with 0.5 vol. % of mid-log phase growth of X513 with 4.45 or 8.90 mM of Cd^{2+} produced the same mixed bio-CdS phases with 17.1 ± 1.4 and 13.0 ± 0.7 nm, respectively. Smaller inocula of X513 delayed the production of H_2S and increased CdS average crystallite size (even for 10 % higher Cd^{2+} dosing) compared to reactions conducted with the conventional 2 % inocula. Under conditions of higher concentration of Cd^{2+} dosing, nucleation of new CdS NP dominated kinetics over the crystal growth [21].

After washing and freeze-drying, the yield of CdS NP was 0.58 ± 0.02 g/L of medium after 12 days with 99.7 ± 3.9 % of the Cd having been incorporated into CdS NP (Table 1). The highest yield of 3.7 ± 0.25 g/L/month CdS NP was achieved among various Cd^{2+} dosing concentrations, times, and aging, but with only 70 ± 4.7 % conversion efficiency.

Scalability of microbially facilitated synthesis of CdS NP was tested for increasing medium volume from 10 mL to a dual 24 L parallel reactor (Fig. 5**a**–**d**) with the same Cd dosing conditions (0.4 mM/day for 10 days). Scaling showed no significant influence on size or optical properties of CdS NP, as evidenced by the same fluorescent luminance (FL) with emissions at 530 nm (Fig. 5**e**). This demonstrated a factor of 2,400 scalability of the microbially facilitated synthesis of CdS NP. The scalability factor was similar to that demonstrated for biomagnetite as it proceeded from 10 mL to 30 L [20]. Increased

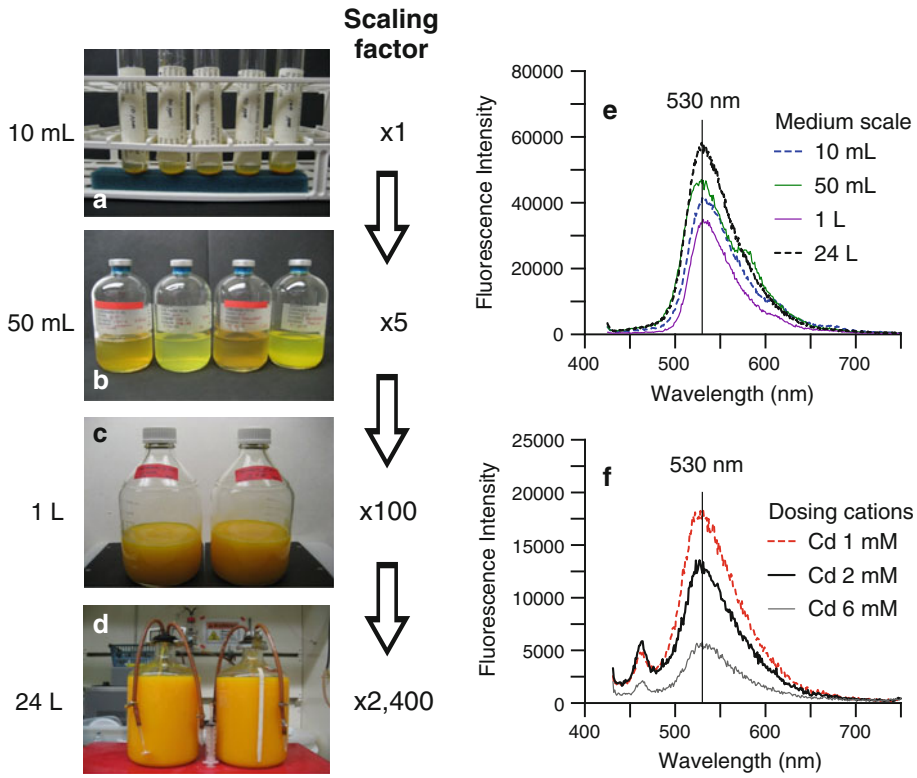

Fig. 5 Scale-up experiment for CdS NP from 10 mL to 24 L; **a** dosing 0.09, 0.27, 0.44, 0.62, and 0.89 mM of Cd^{2+} to 10 mL; **b** pairs of control and microbial samples of 50 mL (*left*, with cysteine S; *right*, with thiosulfate); **c** pulsed dosing of 0.4 and 0.8 mM/day for 10 days to 1 L; **d** pulsed dosing of 0.4 mM/day for 10 days to parallel reactors of 24 L. Fluorescence comparison for the scale-up experiment, **e** dosing of Cd 0.4 mM/day into varying medium scales of 10 mL, 50 mL, 1 L, and 24 L of medium for 10 days; f, single dosing of 1, 2, or 6 mM Cd^{2+} into the same 10 mL medium volume

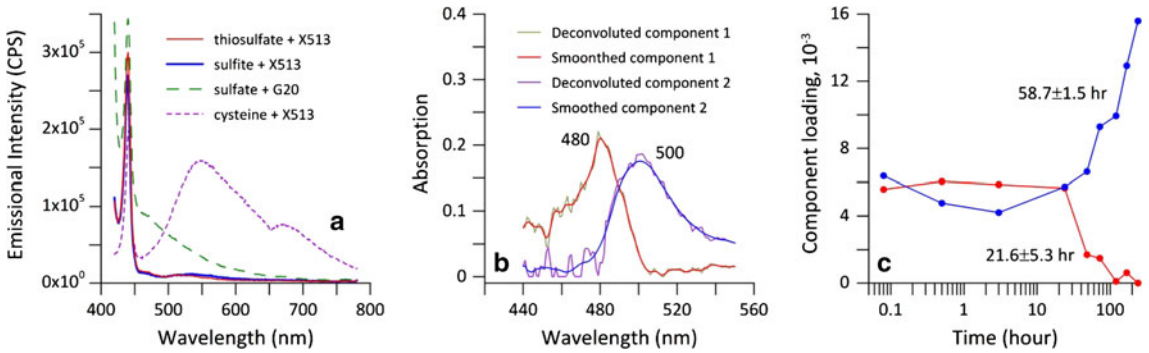

Fig. 6 **a** Photoluminescence spectra of various CdS NP (Excitation at 400 nm); **b**, **c** principal component analysis results exhibiting slow and fast kinetics

dosing concentrations of Cd^{2+} from 1 to 6 mM followed by 3-days incubation did not change the average crystallite size but higher dosing concentrations resulted in lower FL properties (Fig. 5**f**). Results suggested the preferred formation of additional nucleation centers over the crystal growth. The highest FL intensity of CdS NP was observed for a batch inoculated with 1 mM of Cd^{2+} in (Fig. 5**f**). Reduced FL intensity associated with reduced CdS quality might be related to the cation/anion ratios in the medium, which was also related to the production of H_2S.

Optical properties of CdS NP

The photoluminescence (PL) spectra (Fig. 6**a**) with freeze dried samples of CdS NP produced by X513 and thiosulfate or sulfite exhibited a sharp peak around 440 nm, which was also observed in CdS synthesized by standard procedures [37]. The full width at half maximum (FWHM) for Cd NP was found to be ~10 nm, compared to 28 nm [7] or 20 nm FWHM [32] of chemically synthesized CdS, suggesting a narrower size distribution of our CdS NP.

Abiotic reaction with cysteine revealed a PL spectrum of CdS NP showing the same emission peak at 440 nm and a broad band between 450 and 750 nm. This can be attributed to radiative electron and hole relaxation at the defects and impurities on the surface and/or within the CdS NP [7, 30, 37] or charge carriers recombination [32]. The PL spectra with a sharp peak at 440 nm and weak broad emission between 450 and 600 nm was also observed when samples were cultured with G20. This may indicate that microbial fermentation-facilitated CdS NP manufacturing may represent an advantageous route to abiotic reaction in aqueous phase.

Principal component analysis of PL spectra of dried CdS NP shown in Fig. 6**b** revealed two components in solid samples such as relaxation via excitonic transition and surface trap recombination. However, the resulting product from our thiosulfate or sulfite precursors exhibited exciton-dominated PL, in contrast to either samples from the sulfate-reducing bacterium G20, or samples from an abiotic process with sulfide that exhibited a mixed mechanism of surface trap-exciton PL. The analysis of absorption spectra indicated the presence of slow and fast kinetics during the CdS NP synthesis (Fig. 6**b**). The principal component analysis of PL spectra in the solutions revealed that slow kinetics were associated with insignificant changes in the 480 nm component (Fig. 6**c**). At a later time, the 480 nm component loading decreased with a lifetime of $21.6 + 5.9$ h while the 500 nm component loading increased with a longer life time ($58.7 + 1.5$ h). The growth of the second component, likely associated with the large diameter nanoparticles, was not limited by the small nanoparticle seeds (480 nm).

Conclusions

We have demonstrated that thermophilic metal-reducing bacteria can be used to produce CdS NP of controlled size and crystal structure with high yield and size uniformity. Controlling factors such as cell mass, dosing concentrations, type of precursors, and the basal medium composition using appropriate microbial populations as a reducing force were critical in producing copious CdS NP.

Advantages of our CdS NP synthesis using *Thermoanaerobacter* X513 include: (1) a relatively simple procedure without complicated steps [31], (2) low energy consumption at near room temperature compared to traditional methods requiring 250–300 °C [36] or high mechanical energy like ball-milling up to 30 h [25], (3) easily tunable synthetic conditions for size control without implementation of additional steps like anion exchange chromatography [13], (4) semi-continuous production without sacrificing the culture and anaerobic system, (5) minimizing the use of organic solvents and hazardous precursors [9], and (6) no need for post-treatment such as a lengthy dialysis [38].

Stoichiometrically incorporated CdS NP can be easily fabricated into a thin film using the spray or ink-jet method. This process does not require high temperature, an expensive vacuum, or sputtering equipment. The synthetic approach is also not limited to the production of a large surface thin film. Further optimization is underway so as to improve PL of CdS NP and to investigate the influence of other parameters including the concentration of dissolved H_2S, cation/anion ratio, pH, and the monodispersity in the presence of capping agents and surfactants.

Microbially facilitated synthesis processes may offer a novel green technology for low cost, low energy, scalable production of CdS NP with properties comparable to their abiotically synthesized analogs. This approach is not limited to CdS NP, and may be implemented for scalable, cost-effective, green synthesis of other nanoparticles.

Acknowledgments This research was supported by the Department of Energy's (DOE) Advanced Manufacturing Office (AMO), Nanomanufacturing for Energy Efficiency (NT08845) and by the Laboratory Directed Research and Development Program of ORNL (L05512). Part of this research was conducted at the Center for Nanophase Materials Sciences, which is sponsored at the ORNL Scientific User Facilities Division, Office of Basic Energy Sciences, U.S. DOE. The ORNL is managed by UT-Battelle, LLC, for the U.S. DOE under contract DE-AC05-00OR22725. The authors also appreciate James G. Elkins for constructive comments, Tae Hwan Kim for peak analysis, and Sue Carroll for cell counting.

References

1. Bandaranayake RJ, Wen GW, Lin JY, Jiang HL, Sorensen CM (1995) Structural phase behavior in II–VI semiconductor nanoparticles. Appl Phys Lett 67:831–833
2. Bruchez M Jr, Moronne M, Gin P, Weiss S, Alivisatos AP (1998) Semiconductor nanocrystals as fluorescent biological labels. Science 281:2013–2016
3. Chung FH (1974) Quantitative interpretation of X-ray diffraction patterns of mixtures. II. adiabatic principle of X-ray diffraction analysis of mixtures. Appl Cryst 7:519–525
4. Cline JD (1969) Spectrophotometric determination of hydrogen sulfide in natural waters. Limnol Oceanog 14:454–458
5. Cumberland SL, Hanif KM, Javier A, Khitrov GA, Strouse GF, Woessner SM, Yun CS (2002) Inorganic clusters as single source precursors for preparation of CdSe, ZnSe, CdSe/ZnS nanomaterials. Chem Mater 14:1576–1584
6. Dameron CT, Reese RN, Mehra RK, Kortan AR, Carroll PJ, Steigerwald RK, Brus LE, Winge DR (1989) Biosynthesis of cadmium sulphide quantum semiconductor crystallites. Nature 338:596–597
7. Darugar Q, Qian W, El-Sayed MA (2006) Observation of optical gain in solutions of CdS quantum dots at room temperature in the blue region. Appl Phys Lett 88:261108
8. De Azevedo WM, Menezes FD (2012) A new and straightforward synthesis route for preparing CdS quantum dots. J Lumin 132:1740–1743

9. Flenniken M, Allen M, Douglas T (2004) Microbe manufacturers of semiconductors. Chem Biol 11:1478–1480
10. Hummer DR, Kubicki JD, Kent PRC, Post JE, Heaney PJ (2009) The origin of nanoscale phase stability reversals in titanium oxide polymorphs. J Phys Chem C 113:4240–4245
11. Jackson P, Würz R, Rau U, Mattheis J, Kurth M, Schlötzer T, Bilger G, Werner JH (2007) High quality baseline for high efficiency, $Cu(In_{1-x}Ga_x)Se_2$ solar cells. Prog Photovolt: Res Appl 15:507–519
12. Jun Y, Lee S-M, Kang N-J, Cheon J (2001) Controlled synthesis of multi-armed CdS nanorod architectures using monosurfactant system. J Am Chem Soc 123:5150–5151
13. Kang SH, Bozhilov KN, Myung NV, Mulchandani A, Chen W (2008) Microbial synthesis of CdS nanocrystals in genetically engineered *E. coli*. Angew Chem Int Ed 47:5186–5189
14. Labrenz M, Druschel GK, Thomsen-Ebert T, Gilbert B, Welch SA, Kemner KM (2000) Formation of sphalerite (ZnS) deposits in natural biofilms of sulfate-reducing bacteria. Science 290:1744–1747
15. Li Z, Cai W, Sui J (2008) Large-scale preparation of CdS quantum dots by direct thermoysis of a single source precursor. Nanotechnol 19:035602
16. Liu SV, Zhou J, Zhang C, Cole DR, Gajdarziska-Josifovska M, Phelps TJ (1997) Thermophilic Fe(III)-reducing bacteria from the deep subsurface: the evolutionary implications. Science 277:1106–1109
17. Mandal A, Saha J. De G (2011) Stable CdS QDs with intense broadband photoluminescence and high quantum yield. Opt Mater 34:6-11
18. Mi C, Wang Y, Zhang J, Huang H, Xu L, Wang S, Fang X, Fang J, Mao C, Xu S (2011) Biosynthesis and characterization of CdS quantum dots in genetically engineered *Escherichia coli*. J Biotechnol 153:125–132
19. Miller LD, Mosher JJ, Venkateswaran A, Yang ZK, Palumbo AV, Phelps TJ, Podar M, Schadt CW, Keller M (2010) Establishment and metabolic analysis of a model microbial community for understanding trophic and electron accepting interactions of subsurface anaerobic environments. BMC Microbiol 10:149
20. Moon J-W, Rawn CJ, Rondinone AJ, Love LJ, Roh Y, Everett SM, Lauf RJ, Phelps TJ (2010) Large-scale production of magnetic nanoparticles using bacterial fermentation. J Ind Microbiol Biotechnol 37:1023–1031
21. Moon J-W, Rawn CJ, Rondinone AJ, Wang W, Vali H, Yeary LW (2010) Crystallite sizes and lattice parameters of nano-biomagnetie particles. J Nanosci Nanotechnol 10:8298–8306
22. Moon J-W, Roh Y, Lauf RJ, Vali H, Yeary LW, Phelps TJ (2007) Microbial preparation of metal-substituted magnetite nanoparticles. J Microbiol Methods 70:150–158
23. Murasagi A, Nakagawa CW, Hayashi Y (1984) Formation of cadmium-binding peptide allomorphs in fission yeast. J Biochem (Tokyo) 96:1375–1379
24. Navrotsky A (2003) Energetics of nanoparticle oxides: interplay between surface energy and polymorphism. Geochem Trans 4:34–37
25. Patra S, Satpati B, Pradhan SK (2011) Quickest single-step mechanosynthetisis of CdS quantum dots and their microstructure characterization. J Nanosci Nanotechnol 11:4771–4780
26. Roh Y, Liu SV, Li G, Huang H, Phelps TJ, Zhou J (2002) Isolation and characterization of metal-reducing *Thermoanaerobacter* strains from deep subsurface environments of the Piceance Basin, Colorado. Appl Environ Microbiol 68:6013–6020
27. Rondinone AJ, Pawel M, Travaglini D, Mahurin S, Dai S (2007) Metastable tetragonal phase $CdWO_4$ nanoparticles synthesized with a solvothermal method. J Coll Int Sci 306:281–284
28. Smith PR, Holmes JD, Richardson DJ, Russell DA, Sodeau JR (1998) Photophysical and photochemical characterization of bacterial semiconductor cadmium sulfide particles. J Chem Soc, Faraday Trans 94:1235–1241
29. Stürzenbaum SR, Höckner M, Panneerselvam A, Levitt J, Bouillard J-S, Taniguchi S, Dailey LA, Khanbeigi RA, Rosca EV, Thanou M, Suhling K, Zayats AV, Green M (2013) Biosynthesis of luminescent quantum dots in an earthworm. Nature Nanotechnol 8:57–60
30. Tamborra M, Striccoli M, Comparelli R, Curri ML, Petrella A, Agostiano A (2004) Optical properties of hybrid composites based on highly luminescent CdS nanocrystals in polymer. Nanotechnol 15:S240–S244
31. Tong H, Zhu Y-J (2006) Synthesis of CdS nanocrystals based on low-temperature thermolysis of one single source organic metallic precursor. Nanotechnol 17:845–851
32. Uchihara T, Matsumara M, Ono J, Tsubomura H (1990) Effect of ethylenediaminetetraacetic acid on the photocatalytic activities and flat-band potentials of cadmium-sulfide and cadmium selenide. J Phys Chem 94:415–418
33. Wagman DD, Evans WH, Parker VB, Schumm RH, Halow I, Bailey SM, Churney KL, Nuttall RL (1982) J Phy Che Ref Data 11
34. Weimer PJ, van Kavelaar MJ, Michel CB, Ng TK (1988) Effect of phosphate on the corrosion of carbon steel and on the composition of corrosion products in two-stage continuous cultures of *Desulfovibrio desulfuricans*. Appl Environ Microbiol 54:386–396
35. Yao S, Han Y, Liu W, Zhang W, Wang H (2007) Synthesis of CdS nanocrystals with different morphologies via an ultraviolet irradiation route. Mater Chem Phys 101:247–250
36. Yu WW, Peng X (2002) Formation of high-quality CdS and other II–VI semiconductor nanocrystals in noncoordinating solvents: tunable reactivity of monomers. Angrew Chem Int Ed 41:2368–2371
37. Zezza F, Comparelli R, Striccoli M, Curri ML, Tommasi R, Agostiano A (2003) High quality CdS nanocrystals: surface effects. Synth Met 139:597–600
38. Zhang M, Drechsler M, Müller AHE (2004) Template-controlled synthesis of wire-like cadmium sulfide nanoparticle assemblies within core-shell cylindrical polymer brushes. Chem Mater 16:537–543
39. Zhang C, Vali H, Romanek CS, Phelps TJ, Liu SV (1998) Formation of single-domain magnetite by a thermophilic bacterium. Am Miner 83:1409–1418